Journal of Engineering and Applied Sciences 13 (Special Issue 14): 11135-11148, 2018
ISSN: 1816-949X

An Experimental Investigation of Heat Transfer Augmentation of Water-Al_2O_3 Nanofluid Worked Inshell and Helical Coiled Tube Heat Exchanger with Air Bubble Injection Technique

Hameed K. Hamzah, Riyadh S. Al-Turaihi and Anwer A. Abass
Department of Mechanical Engineering, College of Engineering, University of Babylon, Babylon, Iraq

Abstract: In the present research, heat transfer augmentation in shell and helical coiled tube heat exchanger with air bubble injection and Al_2O_3 nanofluid for turbulent flow has been studied. The thermal performance of helical coiled tube heat exchangers has been enhanced with the use of two techniques. The first is represented by air bubble injection in shell side with cold water to enhance the heat transfer rate outside helical coiled tube heat exchanger by creating turbulence in the flowing fluid and the second is represented by adding nanopartical to hot water to produce nanofluid with three volume concentrations (0.1, 0.2 and 0.3%) to increase the heat transfer rate inside the coil. In this research, a new model is designed to mix the air with the water. It ensures that there are small bubbles of water inside the shell and with specific distances to ensure that the excitation is inside the shell. This design was done laboratory and applied and the results were good by examining the number of bubbles and the distance between them by digital camera. The variations of Number of Thermal Units (NTU), exergy loss, dimensionless exergyand effectiveness due to the air bubbles injection with different air flow and fluid flow rate rates are evaluated. The results obtained for all concentrations at different air and nanofluid flow rate were compared with the case when air bubbles were not injected. The outcomes revealed that the heat transfer characteristics enhanced with nanoparticles volumetric concentrations and the air bubble injection. Besides this, water based Al_2O_3 nanofluid with 0.3% of Al_2O_3 nanoparticles gave more enhancement than Al_2O_3 nanofluid with 0.1% of Al_2O_3 nanoparticles as the enhancement in the heat transfer characteristics is directly proportional to the volumetric concentration of nanoparticles in the base fluid. Dependent on air injection condition and Reynolds number, air bubbles increased the amount of Nusselt number about 14-50%. Air bubble injection increased the effectiveness of heat exchanger about 2.5-47.5%.

Key words: Helical coiled tube heat exchanger, nanofluids, heat transfer coefficient, Nusselt number, air bubble, evaluate

INTRODUCTION

Shell and helically coiled-tube heat exchangers are one of the most common equipment found in many industrial applications ranging from solar energy applications, nuclear power production, chemical and food industries, environmental engineering and many other engineering applications. Helical coils are used for transferring heat in chemical reactors and agitated vessels because heat transfer coefficients are higher in it (Saxena and Nigam, 1983). There are various techniques that have been utilized to improve the thermal performance of shell and helical coiltube heat exchangers. The air bubble injection is one such technique to enhance the heat transfer rate. Air bubbles are induced to any flowing fluid channels to maximize the heat transfer characteristics of the fluid. As wall as the different studies, the bubble dynamics causes much impact on the wall skin friction drag. Injecting bubbles in the flowing fluid reduces the density of the liquid that leads to the generation of baroclinic vortices on larger scale. This method can be used in order to improve the performance of any system involving heat transfer process. By Khorasani and Dadvand (2017) thermal properties of fluid are improved when nanopartical mixed with fluid to form a nanofluid, this lead to improve heat transfer rate. Numerous studies have been carried out by researchers to investigate the fluid flow and heat transfer characteristics in the coiled tubes.

Additional applications are showed by Choi and Eastman (Xie *et al*., 2002), Xuan and Li (Abu-Nada *et al*., 2010) and Xie *et al*. (Khodadadi and Hosseinizadeh, 2007). Most liquids like water and oils have low thermal conductivity which can be improved by the addition of

Corresponding Author: Anwer A. Abass, Department of Mechanical Engineering, College of Engineering, University of Babylon, Babylon, Iraq

nanoparticles to the base fluid. Thus, these fluids are called nanofluids and is investigated widely throughout the recent years Abu-Nada *et al.* (Sivasankaran and Pan, 2014). Mukeshkumar *et al.* (2012) and Kannadasan *et al.* (2012) studied the improvement of heat transfer coefficients of shell and helically coiled tube heat exchanger using nanofluid. Saffari *et al.* (2013) experimentally investigated the effect of bubbles on the pressure drop and drag reduction of air-water two phase flows in vertical helical coils. It was found that with the increase of the void fraction, the drag reduction ratio increased and the maximum drag reduction ratio was 25% which occurs at low reynolds numbers. Salimpour (2008) experimentally investigated to study the heat transfer characteristics of a shell and coiled tube heat exchanger with a temperature dependent-property fluid (engine oil) as the working fluid. It was found out that the coil-side heat transfer coefficients of the coiled tubes with larger pitches are less than those of the ones with smaller pitches. Moawed (2011) carried out experimental investigation to evaluatethe forced convection heat transfer coefficient from helical coiled tubes under constant heat flux condition. He developed a general correlation to describe the average Nusselt (Nu) number and found that the average Nusselt number (Nu_m) increases with the increase Diameter ratio (D/d_o). Dizaji *et al.* (2015a, b) studied the effect of flow, thermodynamic and geometrical characteristics on the exergy loss in a vertical shell and coiled tube heat exchanger. It was demonstrated that exergy loss increases with the increase of shell or coil side flow rate. Dimensionless exergy loss depends on C_{min}. Houshmand and Peles (2014) experimentally studied the effect of air bubble flow rate with water flow rate on heat transfer characteristics in a micro channel and reported an enhancement up to 16% in the heat transfer coefficient. Ghorbani *et al.* (Nandan and Sinh, 2016) experimentally evaluated the effects of coil pitch and tube diameters on shell side heat transfer coefficient of a shell and coiled tube heat exchanger. Their findings showed that the effect of tube diameter on shell-side heat transfer coefficient is negligible. Besides, their results indicated that the convection heat transfer coefficient of shell-side increases when the coil pitch increases. The overall heat transfer coefficient of heat exchanger increases as the heat transfer rate increases. Nandan and Singh (Ghorbani *et al.*, 2010) studied the effect of air bubble injection through shell and tube heat exchangers it has been observed that injecting air bubbles throughout the tube enhances the heat transfer rate by 25-40% at different range of the reynolds number. Thakur and Singh (2017) studied the effect of injection of air bubbles through shell and tube heat exchangers. The injection of air bubbles at the tube inlet and throughout the tube with water based Al_2O_3 nanofluids. The heat transfer rate showed an enhancement of about 25-40%. Also the case where air bubbles were injected throughout the tube gave maximum enhancement followed by the cases of injection of air bubbles at the tube inlet and no air bubble injection. Xiao *et al.* (2018) experimentally investigated single-phase and two phase flow pressure drop characteristics in coiled tubes of inner diameters of 12.5 and 14.5 mm. It was indicated in the single-phase that the friction factor increases with curvature ratio. For flow parameter effects on the two-phase friction pressure drop multiplier, the results show that the multiplier decreases with higher system pressure whilst the mass flux and heat flux does not appear to have asignificant influence. From the literature it was concluded that most of the works focused on enhancement of the heat exchanger performance using nanofluid in a tube flow and some recent research's has focused on injecting air with water. The objective of this research is to find out the effect of air bubble injection over the heat transfer characteristics in shell and helical coil tube heat exchangers containing water based Al_2O_3 hot nanofluid ontube side and cold water on shell side. To accomplish heat transfer enhancement, nanofluid required increasing pumping power and the justification of using nanofluid in terms of pumping power is not studied in most of the research paper.

MATERIALS AND METHODS

Experimental set-up: The schematic diagram has been shown in Fig. 1a and the actual setup has been shown in Fig. 1b. The setup consists of the three diferent sections that is test section, hot nanofluid loop section and the cold water loop section. Test section consists of a shell and helical tube heat exchangers. The detailed configuration of the shell and helical tube heat exchanger has been given in Table 1. The 2 thermocouples have been installed at the entrance and the exit of the test section and six thermocouples set at equal distance onthe inner and outer walls of helical tube to record the diferent temperature with an accuracy of 0.01°C.

Experimental apparatus: Figure 1a shows a schematic diagram and Fig. 1b shows a photographic view of thesetup. The main parts of the setup are the cooling unit including cold watertank, radiator expansion valve) the heating unit involving thermostat, electrical heater and hot water tank and the test section comprising a PVC shell and a copper coiled tube. Parallel and counter flow were used through the heat exchanger for all conditions. The geometric specifications of the shell and coiled tube are given in Table 1. Positive displacement reciprocating

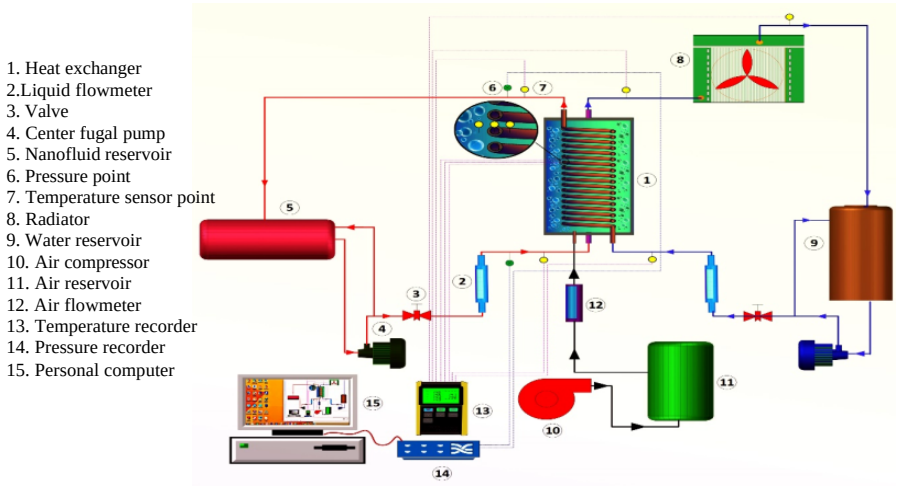

Fig. 1: Schematic diagram of the experimental apparatus

Table 1: Test model (Shell and Helical) specifications

Specifications	Dimensions (mm)
Length of helical tube	620
Thickness of wall	1
Helical tube outer diameter	10
Pitch	20
Number of turn	17
Tuber outer diameter	12.5
Shell length	400
Shell diameter	200
Shell thickness	5

compressor was used to inject the air flow into the cold water flowing through the shell side. Air flow rate was measured using a rota meter (Model DK800S-6), especially designed for volumetric air flow measuring. The temperature measurements were carried out using 12 channels temperature recorder with SD card data recorder (Model BTM-4208SD) having the accuracy ±(0.4%+0.5°C) and the resolution of 0.1°C along with K-type thermocouples. The data logger was calibrated in a 0°C ice water bath to achieve the highest possible accuracy. It showed a temperature of 0.38°C (instead of 0°C) for the ice water bath. In addition, a value of ±0.02°C was added to this value to account for other non-systematic errors (if any). Therefore, the uncertainty of temperature measurement was considered to be ±0.40°C. It should be noted that the temperature of cold water was measured after the air bubbles was totally removed from the cold water at the shell's outlet using a bleeder valve. In addition, the cold water temperature at the shell's inlet was measured before the injection of air bubbles. Air bubbles can be injected with cold water in shell side by radial ports. Therefore, the measured temperatures of the cold water at the shell's inlet and outlet are associated with the pure water. The 2 rotameters type (Flotech) were used to measure the water flow rate. The rotameters were calibrated for both the cold water and hot water using a stopwatch and volumetric flask. At certain times a volumetric flask with a given volume was filled with water and then the amount of water passed through the rotameters was checked. The results were close in both cases for 2 rotameters.

Experiments procedure: Some different conditions considered in this research are presented in Table 2. Each condition was performed with four different cold water (shell side) mass flow rate 25 mm layer of the glass wool insulation were used to prevent heat loss to surrounding from the outer tube (shell). Hot nanofluid with volume concentration 0-0.3% (coiled tube) was maintained at around 60°C and volume flow rate from 1-4 L/min. Cold water (shell side) inlet temperature was maintained at around 23°C and it was pumped inside the shell side of heat exchanger with different water volume flow rate from 1-4 L/min. Air was maintained at around 27°C mixed with cold water at entering shell side at volume flow rate from 1-3 L/min. During the experiments, inlets and outlets bulk temperatures were measured at steady state condition. Both of the parallel flow and counter flow were investigated.

Data processing: To study the effect of air injection in the shell and helical tube heat exchangers, parameters such as overall heat transfer coefficient, heat transfer, exergy loss and dimensionless exergy loss are calculated.

Overall heat transfer coefficient calculation and Nusselt numbers: The average heat transfer rate (Q_{ave}) in a shell and helical tube heat exchanger can be calculated with Eq. 1:

$$Q_c = m_c \times C_{p,c} \times (T_{c,out} - T_{c,in}),\ Q_h = m_h \times C_{p,h} \times (T_{h,in} - T_{h,out}) \quad (1)$$

It is noted that the air mass flow rate (0.0001973 kg/sec) assumed to be negligible compared to the water mass flow rate (at least 0.083 kg/sec) through the test heat exchanger in this study. Indeed, the effect of air mass flow rate on water properties is very small and negligible. Therefore, the effect of air flow rate temperature (if any) was considered negligible. Both counter and parallel flow configurations were examined. The experimental average overall heat transfer coefficient (U_{exp}) in a shell and a helical tube heat exchanger can be obtained by the following correlations (Eq. 2):

$$U_{exp} = \frac{Q_{ave}}{A_0 \Delta T_{LMTD}} \quad (2)$$

Logarithmic temperature difference for parallel flow heat exchanger as Eq. 3:

$$LMTD_{PF} = \frac{\Delta T_1 - \Delta T_2}{In[\Delta T_1 / \Delta T_2]} \quad (3)$$

Where:

$$\Delta T_1 = T_{h,in} - T_{c,in};\ \Delta T_2 = T_{h,out} - T_{c,out}$$

Logarithmic temperature difference for counter flow heat exchanger as Eq. 4:

$$LMTD_{CF} = \frac{\Delta T_1 - \Delta T_2}{In[\Delta T_1 / \Delta T_2]} \quad (4)$$

Where:

$$\Delta T_1 = T_{h,in} - T_{c,out};\ \Delta T_2 = T_{h,out} - T_{c,in}$$

$$\frac{1}{U_o} = \left[\frac{1}{h_o}\right] + \left[\frac{A_i In\left(\frac{Do}{Di}\right)_h}{2\pi k_{cu} L_c}\right] + \left[\frac{A_i}{A_o h_i}\right] \quad (5)$$

The convective heat transfer coefficient at an axial distance 'x' from inlet is given by Eq. 6:

$$h(x) = \frac{q_h}{(T_s(x) - T_b(x)) \times A_s} \quad (6)$$

Where:

q_h = Heat flux from the fluid to wall

$T_s(x)$ = The wall temperature at a distance 'x' from the inlet

$T_b(x)$ = The fluid bulk temperature being measured at a distance 'x' from the inlet

The heat transfer coefficient for helical coil can be calculated by using Eq. 7:

$$q_{h(i)} = m_h \times Cp_h \times (T_{h,i} - T_{h,i+1}) \quad (7)$$

Then, Eq. 8:

$$q_{h(i)} = h_{(i)} A_{s1} (T_s(x) - T_b(x)) \quad (8)$$

Where:

$$A_{s1} = 2\pi r_i L_{(i)} \quad (9)$$

$$h_{(i)} = \frac{q_{h(i)}}{2\pi r_i L_{(i)} \Delta T} \quad (10)$$

where, I is integer from 1-5. For other section of helical coil it has been calculated h_2-h_5. The average heat transfer coefficient (h):

$$h_i = \frac{1}{L}\int_o^L h_x dx \quad (11)$$

Also by same method, the value of h_o is calculated.

Calculation and analysis of NTU: NTU (Number of heat Transfer Units) isindicative of the size of the heat exchanger and it is evaluated by Khorasani and Dadvand (2017), Dizaji *et al.* (2015a, b) (Eq. 12):

$$NTU = \frac{A_o U_{exp}}{C_{min}} \quad (12)$$

where, C_{min} is the minimum thermal capacity and it is defined as:

$$C_h = \dot{m}_h C_{ph},\ C_c = \dot{m}_c C_{pc},\ C_{min} = Min\{C_h \text{ or } C_c\}$$

$$\in = \frac{\text{Actual heat transfer } (Q_{act})}{\text{Maximum heat transfer } (Q_{max})} \quad (13)$$

Maximum possible heat transfer is expressed as:

$$Q_{max} = (\dot{m}c)_{min} \times (T_{h,in} - T_{h,out}) \quad (14)$$

Exergy loss analysis: Generally, exergy is defined as the maximum useful work that can be achieved from the reversible system in a specified environment. When a real device is compared with an actual device in the same flow

and thermal conditions, concepts of reversible work and exergy (availability) are enumerated as significant parameters. For heat exchangers which do not involve shaft work, the exergy given out by one flow is compared with the exergy gained with the other flow. Entropy generation in process is undesirable and it means exergy destruction (Khorasani and Dadvand, 2017; Dizaji *et al*., 2015a, b). The reference environment Temperature (T_∞) in this study is the ambient temperature during the experiments (around 25°C). Temperature difference and pressure drop are two reasons of losses in heat exchangers. In present research, the exergy investigation is based on heat transfer irreversibility. Dimensionless exergy loss (e) was calculated by Akpinar and Bicer study method as described below. For a given steady control volume, exergy balance can be expressed as Eq. 15 (Khorasani and Dadvand, 2017):

$$\sum E_{in} = \sum E_{out} - \sum E_{product} \quad (15)$$

In this study the heat exchanger was adiabatic and it was assumed that the amount of Q_h is equal with the amount Qc. Exergy loss in a steady control volume can be written as follows Eq. 16:

$$E = E_h + E_c \quad (16)$$

E_h and E_c are the exergy change for hot water and cold water, respectively and are calculated as follows Eq. 17:

$$E_h = T_\infty \left\{ \dot{m}_h \left(s_{h,out} - s_{h,in} \right) \right\} \quad (17)$$

$$E_c = T_\infty \left\{ \dot{m}_c \left(s_{c,out} - s_{c,in} \right) \right\} \quad (18)$$

Entropy change can be calculated as Eq. 19:

$$s_{out} - s_{in} = C_{pc} \ln \left(\frac{T_{out}}{T_{in}} \right) \quad (19)$$

Substituting Eq. 19 into Eq. 16-18 yields:

$$E_h = T_\infty \left\{ \dot{m}_h C_{pc} \ln \left(\frac{T_{out}}{T_{in}} \right) \right\} \quad (20)$$

$$E_c = T_\infty \left\{ \dot{m}_c C_{pc} \ln \left(\frac{T_{out}}{T_{in}} \right) \right\} \quad (21)$$

$$E = T_\infty \left\{ \dot{m}_h C_{pc} \ln \left(\frac{T_{out}}{T_{in}} \right) + \dot{m}_c C_{pc} \ln \left[\frac{T_{out}}{T_{in}} \right] \right\} \quad (22)$$

Finally, the dimensionless exergy loss is expressed as follows in Eq. 23:

$$e = \frac{E}{T_\infty C_{min}} \quad (23)$$

Effective thermal properties of nanofluid: The physical properties of nanofluid like thermal conductivity, viscosity, density, specific heat and at various volume fraction of nanoparticles compute by used the following correlations (Lee *et al*., 1999; Pak and Cho, 1998; Brinkman, 1952; Maxwell, 1881).

The effective density of the nanofluid was calculated by using a correlation developed by Lee *et al*. (1999) and Pak and Cho (1998) for nanofluids which is stated as follows (Eq. 24):

$$\rho_{nf} = (1-\varphi)\rho_{bf} + \varphi\rho_p \quad (24)$$

The specific heat of Al_2O_3 nanofluids at different temperatures were estimated for all the volume concentrations considered in the present research, using following equation of Pak and Cho (1998):

$$Cp_{nf} = (1-\varphi)Cp_p + \varphi Cp_{bf} \quad (25)$$

According to Brinkman's formula (Brinkman, 1952), the effective dynamic viscosity of the nanofluid is expressed as:

$$\mu_{nf} = \frac{\mu_{bf}}{(1-\varphi)^{2.5}} \quad (26)$$

The static model of Maxwell (1881) has been used to determine the effective thermal conductivity of liquid-solid suspensions of mono-disperse, low volume-concentration mixtures of spherical particles Eq. 27:

$$k_{nf} = \frac{(k_p + 2k_{bf}) + 2\varphi(k_p - k_{bf})}{(k_p + 2k_{bf}) - \varphi(k_p - k_{bf})} k_{bf} \quad (27)$$

The thermo-physical properties of the base fluid and the considered nanoparticles in this study are given in Table 2 and the effective thermal properties of Al_2O_3-water nanofluid for different concentration are given in Table 3.

Table 2: Properties for Al_2O_3 nanoparticle and base fluid

Variables	ρ (kg/m^3)	C_p (J/kg°C)	k (W/m.°C)	(μkg/m.sec)×10^3
Al_2O_3	3970	765	40	-
Pure water at 60°C	983.3	4179	0.595	0.949

Table 3: Calculation of properties of nanofluid at temperature 60°C

φ	knf (W/m.°C)	nfμ (kg/m.sec)	Cp (nf) (J/kg°C)	ρnf (kg/m^3)	nf(m^2/sec)× 10-7α
0.1	0.617	0.00102	4046.97	1027	1.481
0.2	0.635	0.00113	3922.47	1057	1.531
0.3	0.653	0.00162	3804.87	1087	1.582

RESULTS AND DISCUSSION

Effectiveness of helical heat exchanger: Figure 1 and 2 show relation between effectiveness of helical coil heat exchanger with volume flow rate in shell side. For single phase and two phase flow with air flow rate range from 350-1500 L/h in counter flow direction. It can be noticed the effectiveness increase with increasing flow rate in shell side when hot fluid in coil side is 1 L/min. Also, it has been shown the increasing air flow rate will increase the effectiveness according to Eq. 13, 14 the minimum thermal capacity is hot fluid and it constant at 1 L/min, so that, increase cold water flow rate will increase average heat transfer which increasing the effectiveness. Behavior of air bubble flows together with cold fluid it creates a void which is filled by the fluid surrounding the bubbles. This creates additional turbulence and allows more heat to be carried out from the surfaces by the cooling fluid. Secondly, cold flow volume fraction is reduced by air bubbles injection inside the heat exchanger. For pure water (single phase) the effectiveness slightly increase from 0.2102-0.2724 but for 2 phase flow at 1500 L/h volume flow rate of air, the effectiveness increase with water flow rate from 0.3503 at 1 L/min-0.5609 at L/min. These results may valid to many researchers such as Panahi (2017). Figure 3 indicates the effectiveness variation with water flow rate in shell side for different nanofluid concentration at volume flow rate of air is 500 L/h. It can be observed the adding nanoparticle to water which enhancement the effectiveness of heat exchanger at 4 L/min shell side flow rate, the effectiveness enhances by 54.8 at 0.3 % nanoparticle. Effectiveness increases as volume concentration increase. This due to increase heat transfer coefficient and the nanoparticle causes reduction of temperature difference between the wall and nanofluid according to Eq. 2 the heat transfer rate increase with increase heat transfer coefficient then the increase effectiveness. Figure 4 details effectiveness variation with volume flow rateof cold water in shell side for different air bobble injection flow rate in counter flow direction at hot fluid flow rate 4 L/min. It can be observed that the minimum thermal capacity (C_{min}) in this case is take for cold water in shell side. So that, the effectiveness decrease with increasing flow rate in shell side according to Eq. 13, 14. It has been shown the decrease form (0.554)-(0.325) for 0.1% nanofluid. And have same reason for other concentration. The air bubbles injection volume flow rate which used from 350-1500 LPM in the parallel flow direction as shown in Fig. 5. It has been shown that behavour of parallel flow is similar to counter when hot fluid is less than cold water in shell side. Figure 6 depicts the effectiveness of counter flow is higher than parallel flow because of the smaller size of the bubbles and their greater mobility. In the counter how, hot water enters from the top side of test section and comes down inside the coiled tube. Therefore, when its temperature and capacity have been reduced it has arrived near the bubble's source. However, this event does not occur in parallel how configuration. These results consistent with many papers such as Panahi (2017) (Fig. 3-9).

Specific exergy of helical heat exchange: Figure 7 and 8 illustrate the relation between specific exergy of helical coil heat exchanger with volume flow rate of cold water for single-phase and two-phase flow. The volume

Fig. 2: Photographic view of the setup

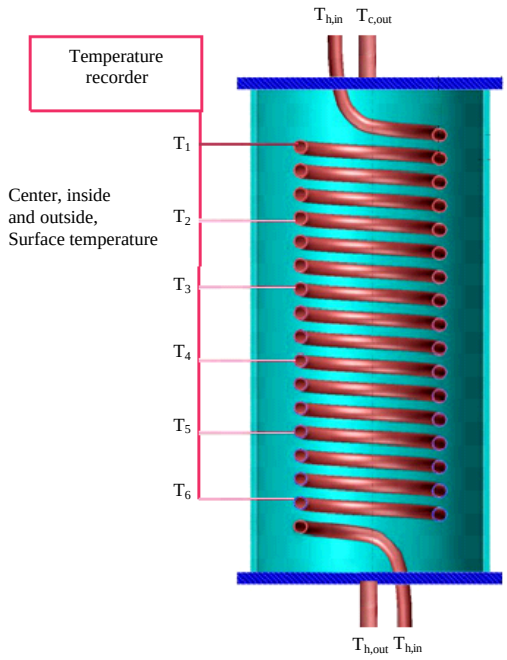

Fig. 3: Distribution temperature in helical coil

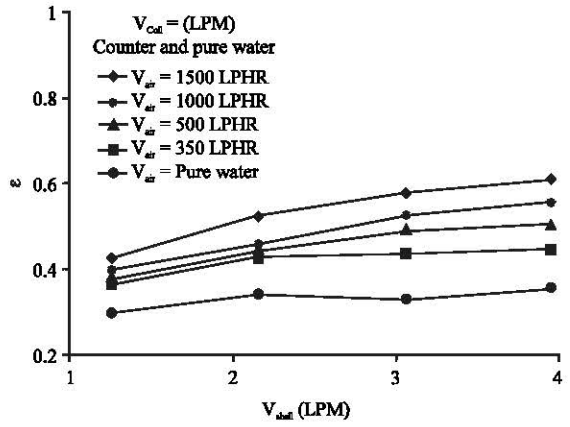

Fig. 4: Variation of effectiveness with volume flowrate of cold water at 1 (L/min) of pure water (CF)

flow rate of cold water has more than that of hot nanofluid volume flow rate, so that, the exergy losses (e) increase with increased volume flow rate of cold water. To this reason, dimensionless exergy loss (e) increase with shell side flow rate depend on Eq. 23. Behavior of air bubble can increase the turbulence level of the shell side water flow. In addition, cold water flow volume rate is reduced by air bubbles injection inside the heat exchanger. For pure water (single phase) the specific exergy slightly increase from 0.005567-0.02781 but for two phase flow at volume flow rate for air = 1500 L/h

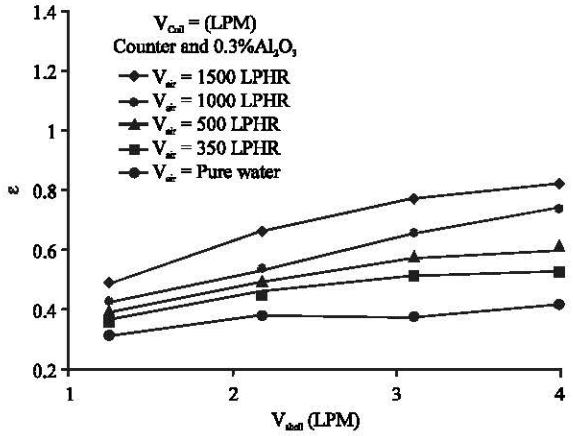

Fig. 5: Variation of effectiveness with volume flowrate cold water at 1 (L/min) of 0.3 % nanofluid (CF)

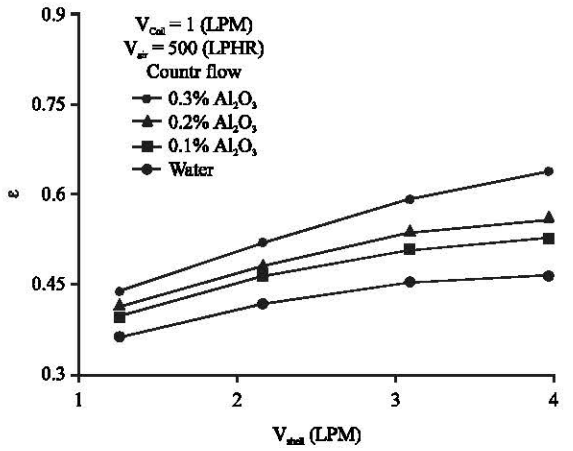

Fig. 6: Variation of effectiveness with volume flowrate cold water at 1 (L/min) and volume concentrations (CF)

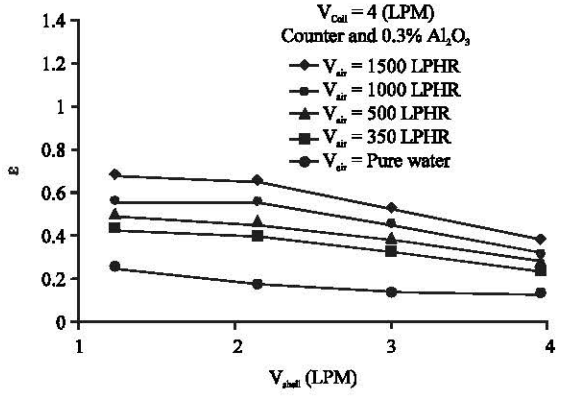

Fig. 7: Variation of effectiveness with volume flowrate cold water at 4 (L/min) and volume concentrations (CF)

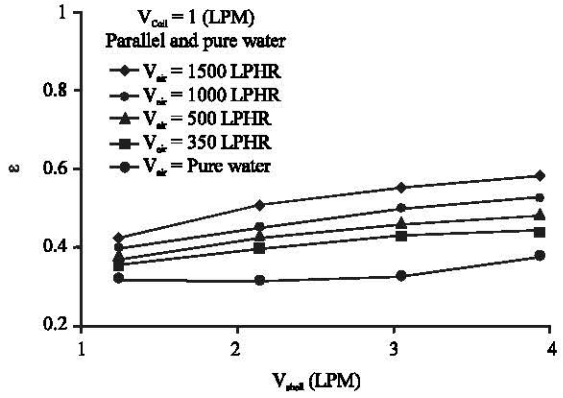

Fig. 8: Variation of effectiveness with volume flowrate cold water at 1 (L/min) of pure water coil side (PF)

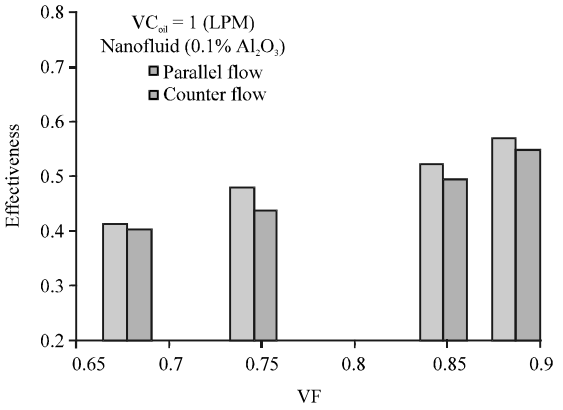

Fig. 9: Amount of effectiveness with volume air fraction for both CF and PF

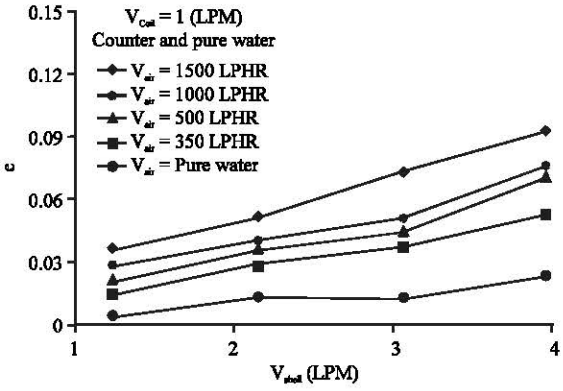

Fig. 10: Variation of specific exergy with volume flowrate cold water at 1 (L/min) of pure water (CF)

the specific exergy increase with water flow rate from 00.04188 at 1 L/min-0.1076 at 4 L/min. Figure 9 indicates the specific exergy variation with cold water flow rate at

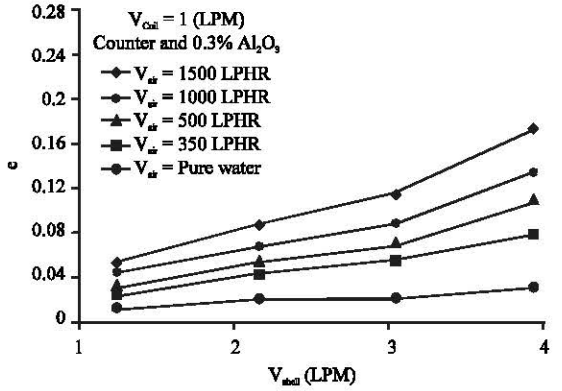

Fig. 11: Variation of specific exergy with volume flowrate of cold water at 1 (LPM) for 0.3% nanofluid (CF)

different nanofluid concentration. It can be observed the adding nanoparticle to water which enhancement the specific exergy of heat exchanger at 4 L/min cold water flow rate where the specific exergy enhances by 68.05 % at 0.3 % nanofluid. Specific exergy increase with increasing of volume concentration. This increment due to increasing of thermal conductivity for nanofluid and decreasing the thickness of thermal boundary layer then temperature difference decrease, so, the exergy loss rate increase according to Eq. 22. It can be observed that according to Fig. 10, the minimum thermal Capacity (C_{min}) in this ease is for cold water in shell side. So that, the specific exergy decrease with increasing flow rate in shell side as stated in Eq. 23. It can be noticed the decrease form (0.1322)-(0.03844) for 0.1 % nanofluid and 1500 L/h air flowrate. And have same reply for other concentration. It can be observed according to Fig. 11, the increase specific exergy with increase nanopartical concentration that due to increase heat transfer coefficient after adding nanoparticles that increase heat transfer rate the specific exergy increase. Figure 12 noticed the specific exergy of counter flow is higher than parallel flow for the same reasons mentioned previously (Fig. 10-15).

Number of Thermal Unit (NTU) of helical heat exchanger: Figure 13 and 14 include the variation between NTU of helical coil heat exchanger with volume flow rate in shell side, air flow rate range from 350-1500 L/h in counter flow direction. It can be observed the NTU increase with increasing flow rate in shell side when hot fluid in coil side is 1 L/min. Minimum thermal Capacity (C_{min}) for hot fluid and it is constant at 1 L/min. When cold water flow rate in shell side will be increase. NTU value increase from (0.3277) at 1 L/min to

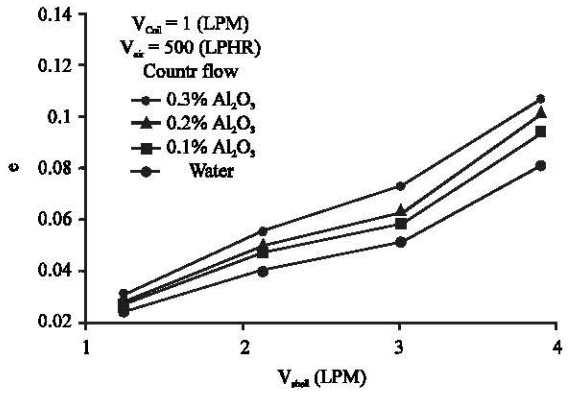

Fig. 12: Variation of specific exergy with volume flowrate of cold water at 1 (L/min) and volume concentrations (CF)

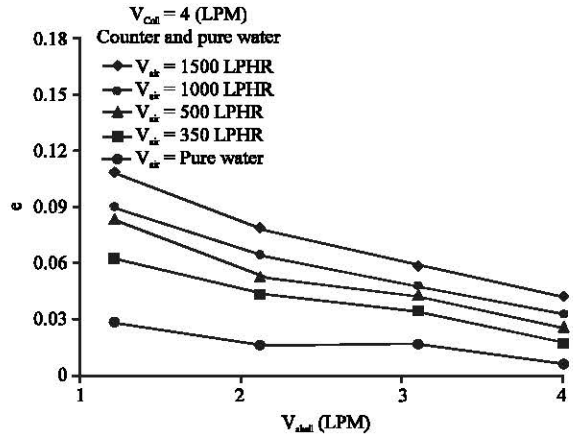

Fig. 13: Variation of specific exergy with volume flowrate of cold water at 4 (L/min) for pure hot water (CF)

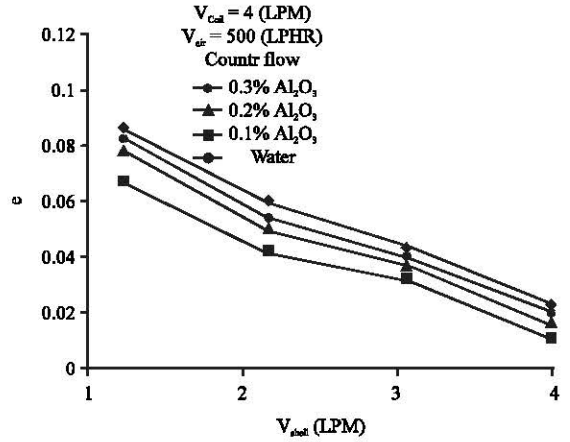

Fig. 14: Variation of specific exergy with volume flowrate cold water at 4 (L/min) and volume concentrations (CF)

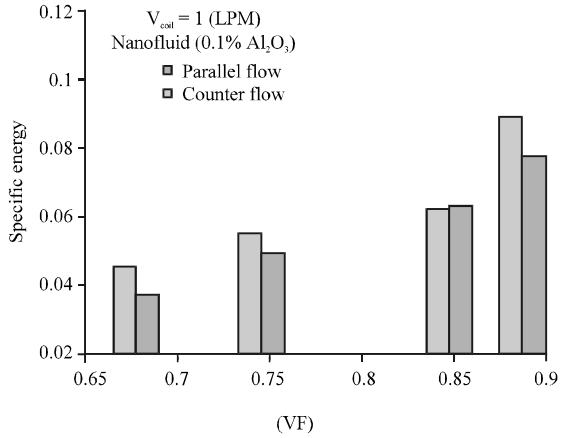

Fig. 15: Amount of specific exergy with volume air fraction for CF and PF

(0.3507) at 4 L/min for pure water. Also, NTU value increase from (0.4725) at 1 L/min to (0.6073) at 4 L/min for 0.3% nanofluid. Figure 15 illustrate that adding nanoparticle to water which enhancement the NTU of heat exchanger at 4 L/min cold water flow rate, the NTU enhance by 68.7 % in 0.3 % nanofluid. NTU increase as volume concentration increase. This due to increase thermal conductivity by reduce temperature different between wall and bulk temperature that increase overall heat transfer. Figure 16 show that the minimum thermal capacity in the case that range of cold water form (1-4 L/min) and flow rate of hot nanofluid is 4L/min. As volume flow rate of cold water increases NTU will be decreases, this get depending on (Eq. 3-12). Also when air volume flow rate increases the NTU improve from (0.004077) at1 L/min to (0.03844) at 4 L/min at for flow rate of hot nanofluid is 4 L/min. 0.1 % volume concentration. Figure 17 states improve NTU values as volume concentration increase. NTU values increase form (0.7442)-(1.798) for 500 L/h air flow rate and 4 L/min hot water flow rate and have same behavior for other concentration. Figure 18 illustrated the NTU values of counter flow is higher than parallel flow for the same reasons mentioned previously (16-22).

Nusselt number of helical heat exchanger: Figure 19-23 demonstrate that the Nusselt number increase with increasing flow rate of cold water for all values of air flow rate and Nusselt number values increase as concentrations increase. This is due to two reasons, first when the volume concentrations increased, the thermal conductivity of nanofluid increased, the number of nanoparticles increased and hence their total contact area was simply higher which in turn would provide a more

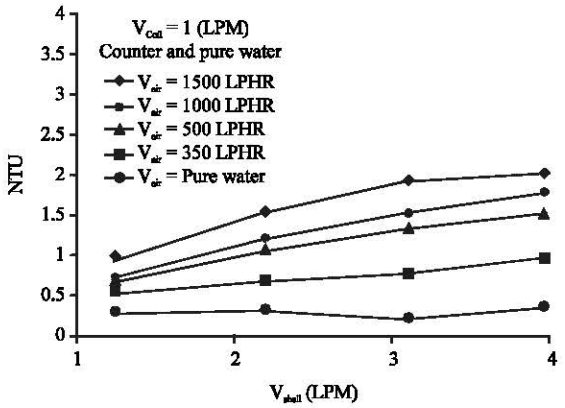

Fig. 16: Variation of NTU with volume flowrate of cold water s at 1 (L/min) for pure water (CF)

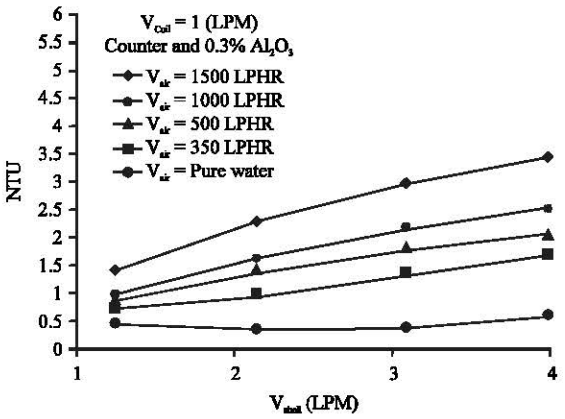

Fig. 17: Variation of NTU with volume flowrate of cold water at 1 (L/min) for 0.3 % nanofluid (CF)

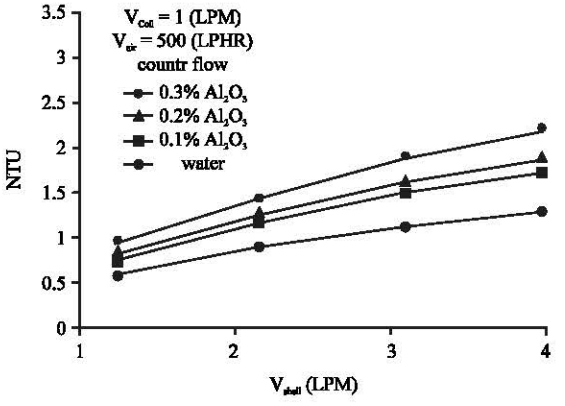

Fig. 18: Variation of NTU with volume flowrate of cold water at 1 (L/min) and volume concentration (CF)

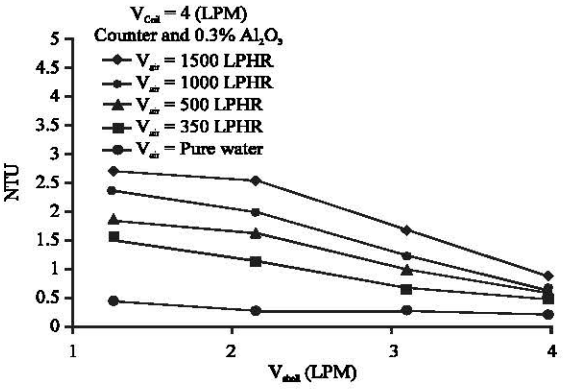

Fig. 19: Variation of NTU with volume flowrate of cold water at 4 (L/min) for 0.3% nanofluid (CF)

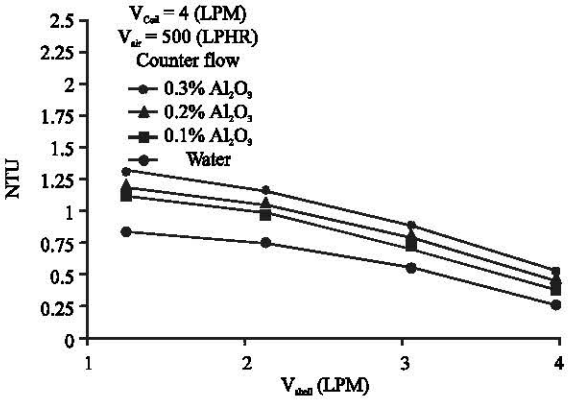

Fig. 20: Variation of NTU with volume flowrate of cold water shell side at 4 (L/min) and volume concentrations (CF)

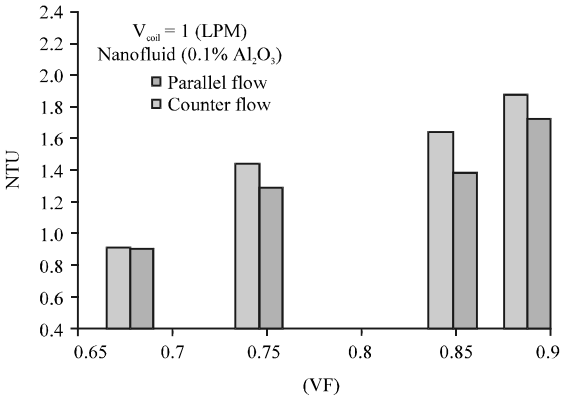

Fig. 21: Amount of NTU with volume fraction for CF and PF

effective heat exchange between the nanoparticles and base fluid. Secondly that when the concentrations of nanofluid increased, the viscosity and density of nanofluid increased, number of nanopartical increased, this deals with the collisions between the nanofluid and

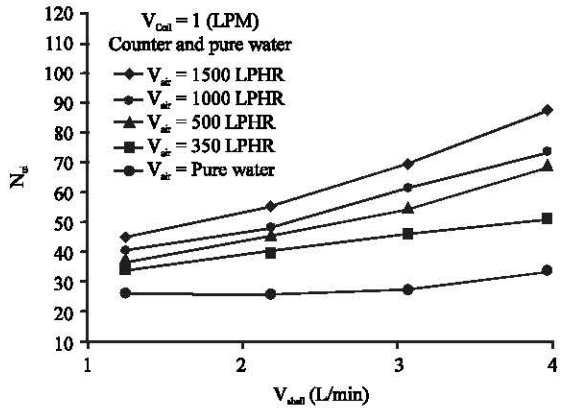

Fig. 22: Variation of Nusselt number with volume flowrate of cold water at 1 (L/min) for pure water (CF)

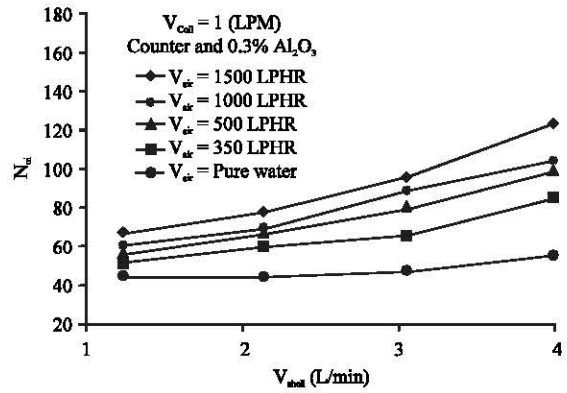

Fig. 23: Variation of Nusselt Number with volume flowrate of cold water 1 (L/min) for 0.3 % nanofluid (CF)

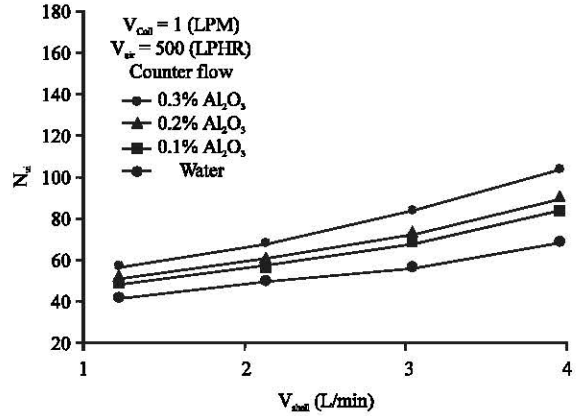

Fig. 24: Variation of Nusselt Number with volume flowrate of cold water at 1 (L/min) and volume concentration (CF)

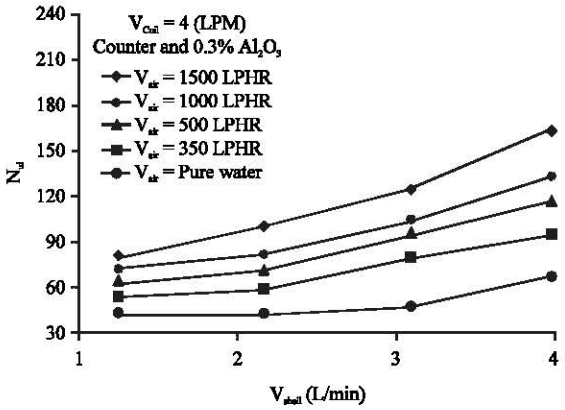

Fig. 25: Variation of Nusselt Number with volume flowrate of water shell side at 4 (L/min) for 0.3% nanofluid (CF)

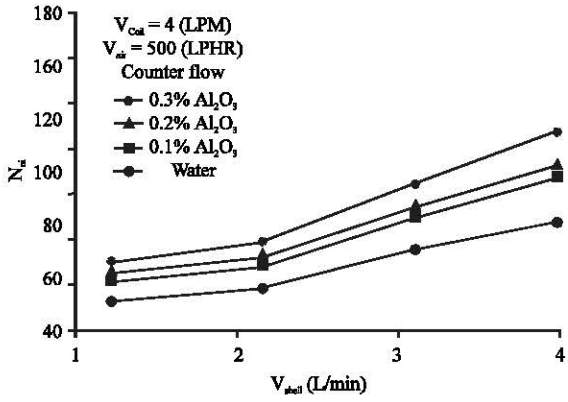

Fig. 26: Variation of Nusselt Number with volume flowrate of water shell side at 4 (L/min) and volume concentrations (CF)

the pipe wall increased. Figure 24 illustrated the NTU values of counter flow is higher than parallel flow for the same reasons mentioned previously (Fig. 23-29).

Figure 25 show that flow rate of hot water increase the pressure drop increased and for same flow rate value, the value of pressure drop increased with concentration of nanofluid increased. This is due to three reasons, firstly that when flow rate increase the pressure values increased, the friction factor decreased. This led to the pressure drop to be increased and secondly that when the concentrations of nanofluid increased the pressure values decreased because increased viscosity and density of nanofluid, so, the friction factor increased. This led to pressure drop to be decreased, 3rd reasons, the collisions between the particles of nanofluid and between the particles and wall of coil, this caused an obstruction to the

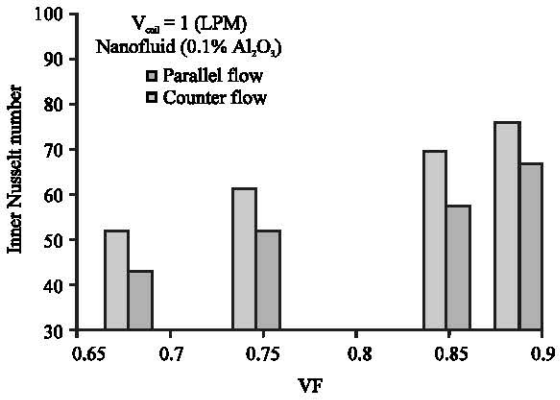

Fig. 27: Amount of Nusselt number with volume air fraction for CF and PF

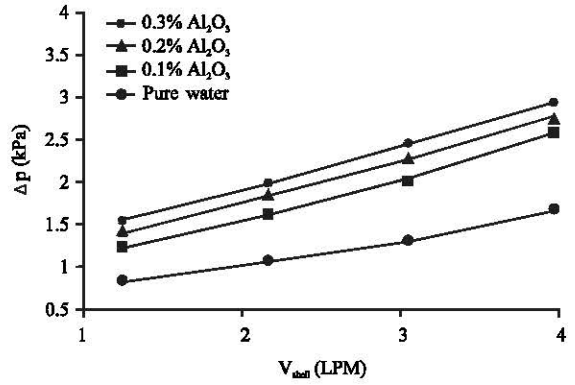

Fig. 28: Variation of pressure drop with tube side volume flow rate

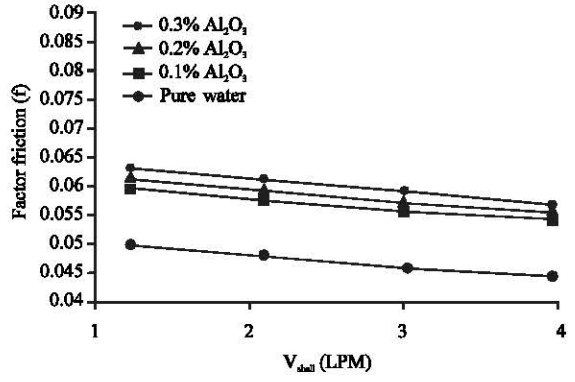

Fig. 29: Comparison between friction factor for different nanoparticle concentration

fluid flow. The results closed to many papers such as (Fotukian and Esfahany, 2010). Figure 26 illustrate that when volume concentrations increased the friction factor increased and for same values of volume concentrations. The friction factor values increased as nanofluid flow rates decreased. This is due to the same reasons. The results closed to many papers such as Arani and Amani (2013).

CONCLUSION

Some important conclusions from the study are provided as: The experimental results indicate that Nusselt number (Nu) was increased by increasing particles volume concentrations and Reynolds number.

It was observed that the pressure drop of nanofluid has not significant increase compared to distillated water for volume concentrations less 0.2% but the pressure drop increase for volume concentrations more than 0.2%.

Dependent on air injection condition and Reynolds number, air bubbles increased the amount of nusselt number about 6-35%. Air bubble injection increased the effectiveness of heat exchanger about 10-40%.

The bubble generation can improve the heat transfer rate about 30% for some cases and the other cases require an adjustment process by controlling the air injection rates (bubble generation) for obtaining the better results according to the operating conditions.

Dependent on air injection condition and cold water mass flow rate (shell side) an increase of up to 1.5-4.2 times in NTU, 1.23-2.59 times in dimensionless exergy loss and 1.36-2.44 in effectiveness compared to the pure water (without bubble injection) were obtained.

It is studied that the overall heat transfer coefficient of counter flow is 4-8% higher than that of parallel flow at 0.3% nanofluid. The overall heat transfer coefficient is 5-9% higher than that of parallel flow at 0.8% nanofluid.

NOMENCLATURE

A	=	Area (m^2)
C_p	=	Specific heat (J/kg.°C)
D	=	Diameter (m)
F	=	Friction factor
K	=	Thermal conductivity (W/m °C)
L	=	Length of pipe (m)
M	=	Mass (kg)
Nu	=	Nusselt number
Q	=	Amount of heat transfer (W)
P	=	pressure (N/m^2)
R	=	Radius of pipe (m)
Re	=	Remolds number
T	=	Temperature (°C)
U	=	Velocit (m/sec)

Greek symbols:

μ	=	Dynamic viscosity (kg/m.sec)
V	=	Volume flow rate (m^3/sec)

ρ = Density (kg/m^3)
φ = Volume concentration (%)

Subscripts:

bf = Bace fluid
f = liquid phases
in = Inlet
nf = Nanofluid
out = Outlet
p = Solid particle
s = Surface

REFERENCES

Abu-Nada, E., Z. Masoud, H.F. Oztop and A. Campo, 2010. Effect of nanofluid variable properties on natural convection in enclosures. Intl. J. Therm. Sci., 49: 479-491.

Arani, A.A. and J. Amani, 2013. Experimental investigation of diameter effect on heat transfer performance and pressure drop of TiO_2-water nanofluid. Exp. Therm. Fluid Sci., 44: 520-533.

Brinkman, H.C., 1952. The viscosity of concentrated suspensions and solutions. J. Chem. Phys., 20: 571-581.

Dizaji, H.S., S. Jafarmadar and M. Hashemian, 2015. The effect of flow, thermodynamic and geometrical characteristics on exergy loss in shell and coiled tube heat exchangers. Energy, 91: 678-684.

Dizaji, H.S., S. Jafarmadar, M. Abbasalizadeh and S. Khorasani, 2015. Experiments on air bubbles injection into a vertical shell and coiled tube heat exchanger; exergy and NTU analysis. Energy Convers. Manage., 103: 973-980.

Fotukian, S.M. and M.N. Esfahany, 2010. Experimental investigation of turbulent convective heat transfer of dilute ?-Al_2O_3/water nanofluid inside a circular tube. Intl. J. Heat Fluid Flow, 31: 606-612.

Ghorbani, N., H. Taherian, M. Gorji and H. Mirgolbabaei, 2010. Experimental study of mixed convection heat transfer in vertical helically coiled tube heat exchangers. Exp. Therm. Fluid Sci., 34: 900-905.

Houshmand, F. and Y. Peles, 2014. Impact of flow dynamics on the heat transfer of bubbly flow in a microchannel. J. Heat Transfer, 136: 1-8.

Kannadasan, N., K. Ramanathan and S. Suresh, 2012. Comparison of heat transfer and pressure drop in horizontal and vertical helically coiled heat exchanger with CuO/water based nano fluids. Exp. Therm. Fluid Sci., 42: 64-70.

Khodadadi, J.M. and S.F. Hosseinizadeh, 2007. Nanoparticle-Enhanced Phase Change Materials (NEPCM) with great potential for improved thermal energy storage. Intl. Commun. Heat Mass Transfer, 34: 534-543.

Khorasani, S. and A. Dadvand, 2017. Effect of air bubble injection on the performance of a horizontal helical shell and coiled tube heat exchanger: An experimental study. Appl. Therm. Eng., 111: 676-683.

Lee, S., S.U.S. Choi, S. Li and J.A. Eastman, 1999. Measuring thermal conductivity of fluids containing oxide nanoparticles. J. Heat Transfer, 121: 280-289.

Maxwell, J.C., 1881. A Treatise on Electricity and Magnetism. 2nd Edn./Vol. 1, Clarendon Press, England, UK., Pages: 464.

Moawed, M., 2011. Experimental study of forced convection from helical coiled tubes with different parameters. Energy Convers. Manage., 52: 1150-1156.

Mukeshkumar, P.C., J. Kumarb, S. Suresh and K.P. Babu, 2012. Experimental study on parallel and counter flow configuration of a shell and helically coiled tube heat exchanger using Al2O3/water nanofluid. J. Mater. Environ. Sci., 3: 766-775.

Nandan, A. and G. Sinh, 2016. Experimental study of heat transfer rate in a shell and tube heat exchanger with air bubble injection. Intl. J. Eng. Trans. B., 29: 1160-1166.

Pak, B.C. and Y.I. Cho, 1998. Hydrodynamic and heat transfer study of dispersed fluids with submicron metallic oxide particles. Exp. Heat Transfer, 11: 151-170.

Panahi, D., 2017. Evaluation of Nusselt number and effectiveness for a vertical shell-coiled tube heat exchanger with air bubble injection into shell side. Exp. Heat Transfer, 30: 179-191.

Saffari, H., R. Moosavi, E. Gholami and N.M. Nouri, 2013. The effect of bubble on pressure drop reduction in helical coil. Exp. Therm. Fluid Sci., 51: 251-256.

Salimpour, M.R., 2008. Heat transfer characteristics of a temperature-dependent-property fluid in shell and coiled tube heat exchangers. Intl. Commun. Heat Mass Transfer, 35: 1190-1195.

Saxena, A.K. and K.D.P. Nigam, 1983. Effect of coil pitch and cross-sectional ellipticity on RTD for diffusion-free laminar flow in coiled tubes. Chem. Eng. Commun., 23: 277-289.

Sivasankaran, S. and K.L. Pan, 2014. Natural convection of nanofluids in a cavity with nonuniform temperature distributions on side walls. Numer. Heat Transfer Part A. Appl., 65: 247-268.

Thakur, G. and G. Singh, 2017. An experimental investigation of heat transfer characteristics of water based Al_2O_3 nanofluid operated shell and tube heat exchanger with air bubble injection technique. Intl. J. Eng. Technol., 6: 83-90.

Xiao, Y., Z. Hu, S. Chen and H. Gu, 2018. Experimental study of two-phase frictional pressure drop of steam-water in helically coiled tubes with small coil diameters at high pressure. Appl. Therm. Eng., 132: 18-29.

Xie, H., J., Wang, T. Xi, Y. Liu and F. Ai, 2002. Dependence of the thermal conductivity of nanoparticle-fluid mixture on the base fluid. J. Mater. Sci. Lett., 21: 1469-1471.